Electronic Supplementary Material (ESI) for Journal of Materials Chemistry A.

Supplementary Information

Sulfur-doped cobalt molybdenum oxide with hydrangea-like structure for bi-functionally efficient overall water splitting

Jie Dong,[a] Saiyi Chen,[a] Cuncai Lv,[b] Mark G Humphrey,[c] Chi Zhang[a,*] and Zhipeng Huang[a,*]

[a] China-Australia Joint Research Center for Functional Molecular Materials, School of Chemical Science and Engineering, Tongji University, Shanghai, 200092, China. Email: chizhang@tongji.edu.cn, zphuang@tongji.edu.cn

[b] Key Laboratory of High-precision Computation and Application of Quantum Field Theory of Hebei Province, Hebei Key Lab of Optic-electronic Information and Materials, The College of Physics Science and Technology, Hebei University, Baoding 071002, China

[c] Research School of Chemistry, Australian National University, Canberra, ACT, 2601, Australia

The specific steps of HER are as follows:

$H_2O + M + e^- \rightleftharpoons MH_{ads} + OH^-$ （Volmer step）

$MH_{ads} + H_2O + e^- \rightleftharpoons M + H_2 + OH^-$ （Heyrovsky step）

$2MH_{ads} \rightleftharpoons 2M + H_2$ (Tafel step)

where M is the catalyst active site, and ads are chemisorption.

The specific steps of OER are as follows:

$^* + OH^- \rightarrow {}^*OH + e^-$

$^*OH + OH^- \rightarrow H_2O + {}^*O + e^-$

$^*O + OH^- \rightarrow {}^*OOH + e^-$

$^*OOH + OH^- \rightarrow {}^* + O_2 + e^-$

where * is the catalyst's active site.

Kinetic analysis based on the dual-pathway kinetic model: [1,2]

Based on the Tafel-Heyrovsky-Volmer mechanism, there are three elementary reaction steps for the HOR-HER (with + and − for the reactions in the HOR and HER direction) on the catalysts' surfaces.

$H_2O + e^- \rightleftharpoons H_{ads} + OH^-$ (Volmer, V)

$H_{ads} + H_{ads} \rightleftharpoons H_2$ (Tafel, T)

$H_2O + H_{ads} + e^- \rightleftharpoons H_2 + OH^-$ (Heyrovsky, H)

For the HER process, the total kinetic currents (J_k) can be expressed as:

$J_k = J_T + J_H = J_V - J_T$

Where the kinetic currents for J_T, J_V, and J_H are:

$$J_T = J_{+T} - J_{-T} = J^* e^{-\Delta G^{*0}_{+T}/kT}[(1-\theta)^2 - e^{2\Delta G^0_{ad}/kT}\theta^2]$$

$$J_V = J_{+V} - J_{-V} = J^* e^{-\Delta G^{*0}_{-V}/kT}[e^{(\Delta G^0_{ad}+0.5\eta)/kT}\theta - e^{-0.5\eta/kT}(1-\theta)]$$

$$J_H = J_{+H} - J_{-H} = J^* e^{-\Delta G^{*0}_{+H}/kT}[e^{0.5\eta/kT}(1-\theta) - e^{\Delta G^0_{ad}-0.5\eta/kT}\theta]$$

where the fixed reference prefactor j^* is 1000 A cm^{-2}

The four variable kinetic parameters are the standard (at zero overpotential) free energies of adsorption for the reaction intermediate, H_{ad} (ΔG^0_{ad}), and ΔG^{*0}_{+T} for Tafel step, ΔG^{*0}_{-V} for Volmer step, ΔG^{*0}_{+H} for Heyrovsky step. The adsorption isotherm, θ, can be expressed as:

$$\theta = \frac{-B-\sqrt{B^2-4AC}}{2A}$$

In which

$A = 2g_{+T} - 2g_{-T}$

$B = -4g_{+T} - g_{+H} - g_{-H} - g_{+V} - g_{-V}$

$C = 2g_{+T} + g_{+H} + g_{-V}$

The expressions for g_i are given below:

$g_{+T} = \exp(-\Delta G^{*0}_{+T}/kT)$

$g_{-T} = \exp[-(\Delta G^{*0}_{+T} - 2\Delta G^0_{ad})/kT]$

$g_{+V} = \exp[-(\Delta G^{*0}_{-V} - \Delta G^0_{ad} - 0.5\eta)/kT]$

$g_{-V} = \exp[-(\Delta G^{*0}_{-V} + 0.5\eta)/kT]$

$g_{+H} = \exp[-(\Delta G^{*0}_{+H} - 0.5\eta)/kT]$

$g_{-H} = \exp[-(\Delta G^{*0}_{+H} - \Delta G^0_{ad} + 0.5\eta)/kT]$

where kT = 25.51 meV at 296.15 K

Content

conditions.

Table S5 XPS peak positions and percent peak areas of fitted high-resolution spectra of Co 2p, Mo 3d, O 1s and S 2p for CoMoO and S-CoMoO-12.4.

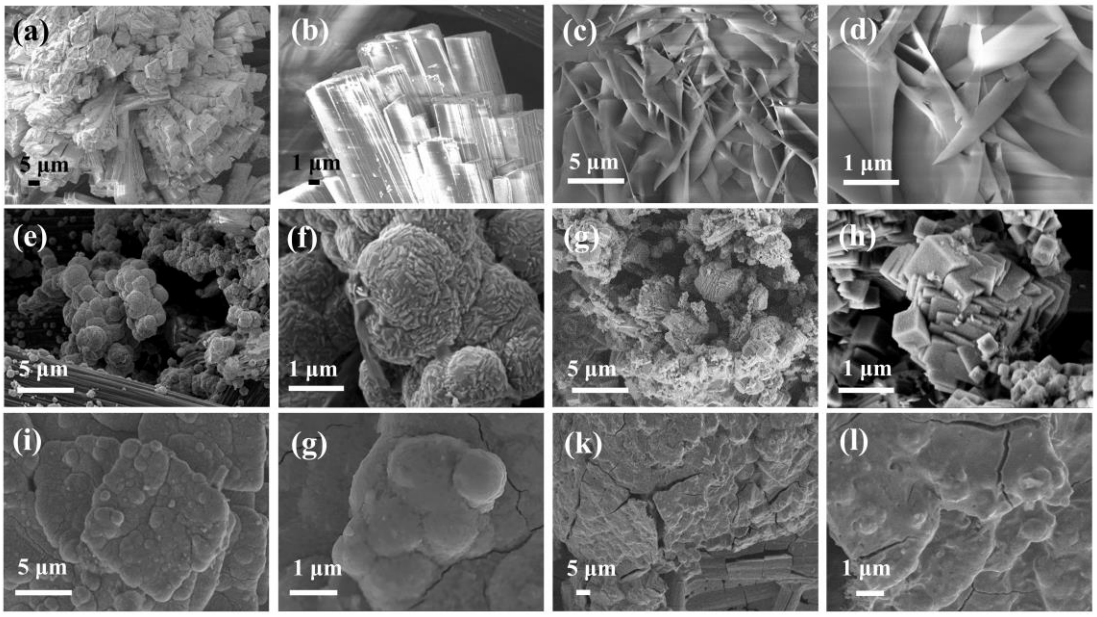

Fig. S1 SEM images of (a, b) CoMoO, (c, d) S-CoMoO-3.1, (e, f) S-CoMoO-6.2, (g, h) S-CoMoO-9.3, (i, g) S-CoMoO-15.5 and (k, l) S-CoMoO-18.6 samples.

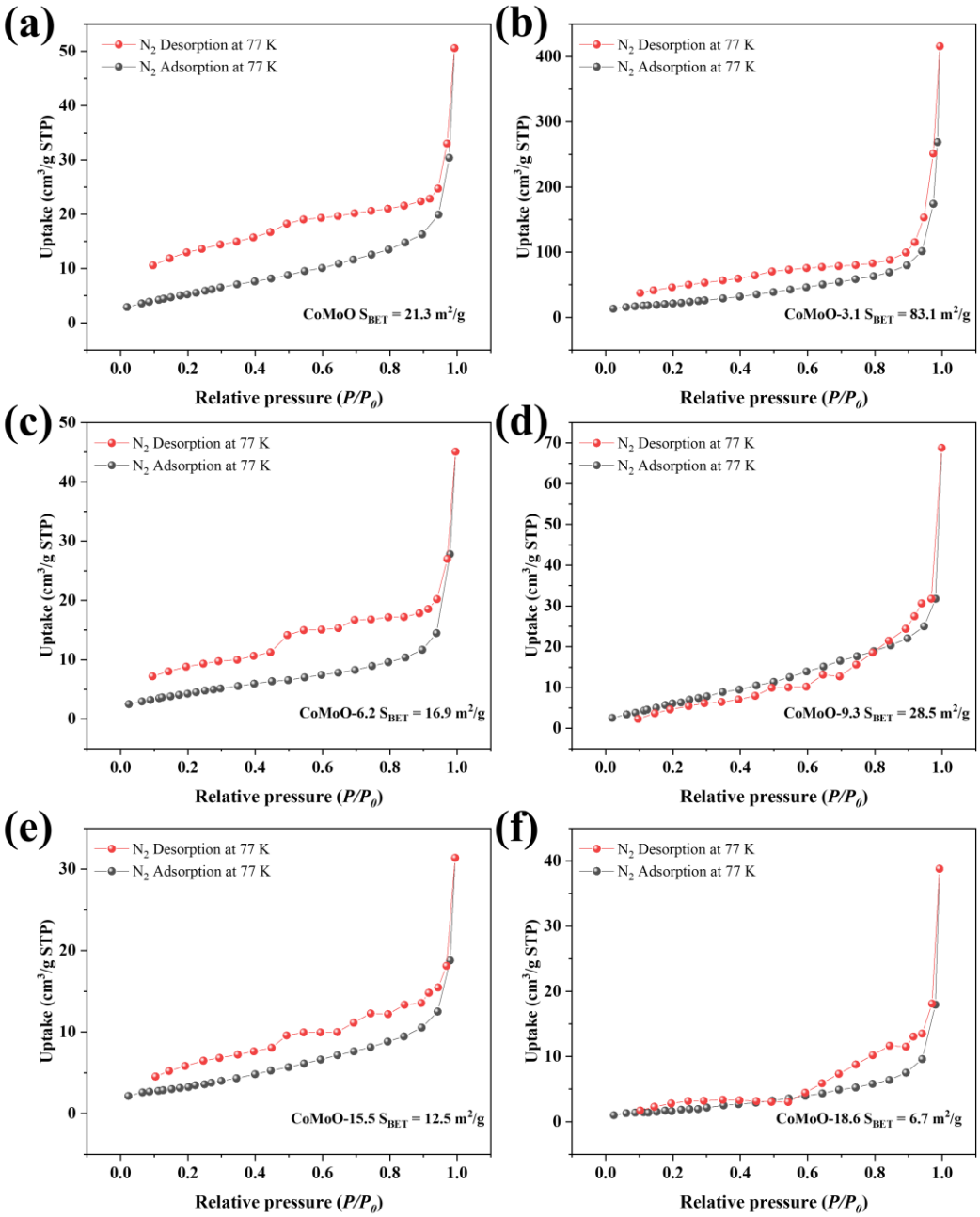

Fig. S2 N_2 sorption isotherms of (a) CoMoO, (b) S-CoMoO-3.1, (c) S-CoMoO-6.2, (d) S-CoMoO-9.3, (e) S-CoMoO-15.5 and (f) S-CoMoO-18.6 samples.

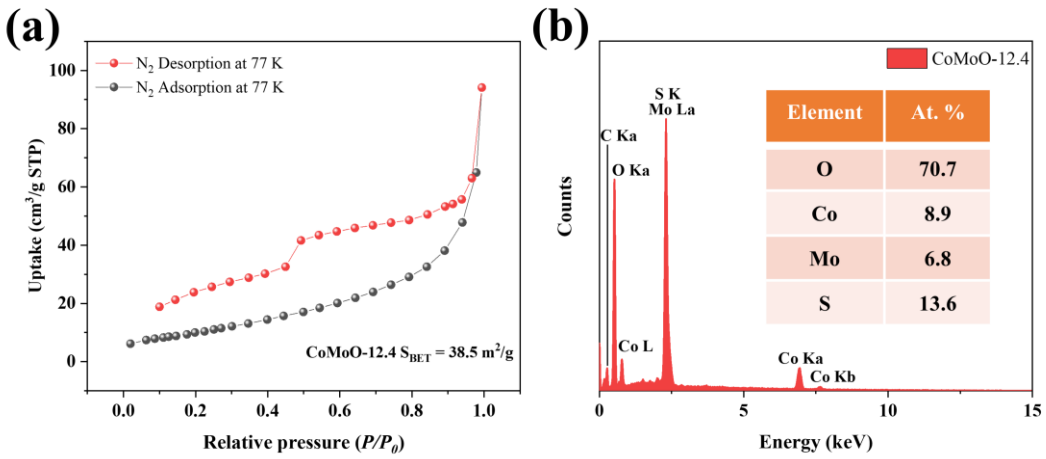

Fig. S3 (a) N_2 sorption isotherms of S-CoMoO-12.4; (b) EDS spectrum and elemental analysis data of S-CoMoO-12.4.

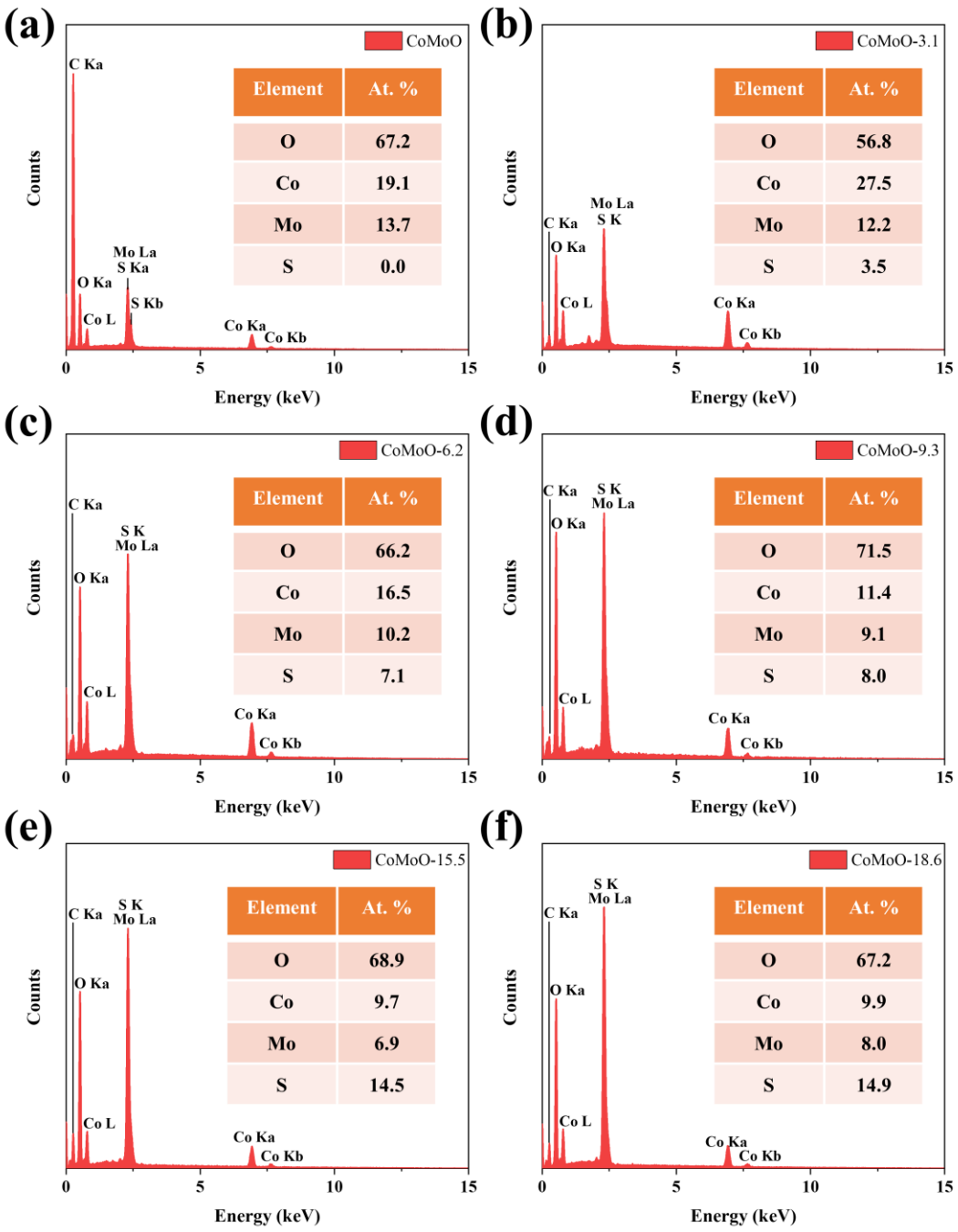

Fig. S4 EDS spectra and elemental analysis datas of (a) CoMoO, (b) S-CoMoO-3.1, (c) S-CoMoO-6.2, (d) S-CoMoO-9.3, (e) S-CoMoO-15.5 and (f) S-CoMoO-18.6 samples.

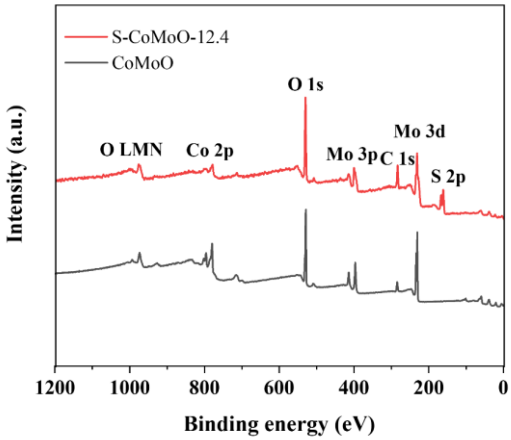

Fig. S5 XPS survey spectra of CoMoO and S-CoMoO-12.4.

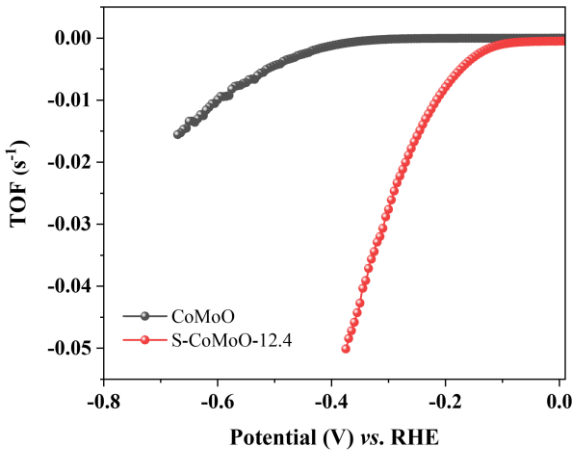

Fig. S6 The calculated TOF (HER) curves of CoMoO and S-CoMoO-12.4.

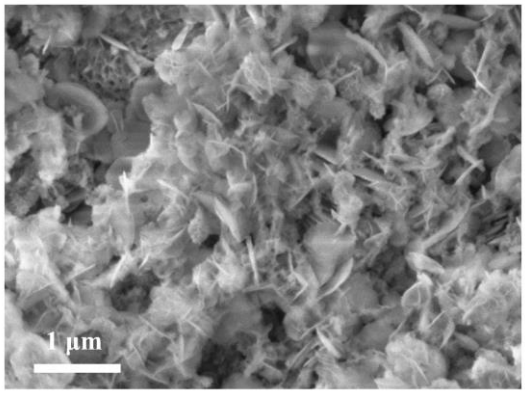

Fig. S7 SEM images of S-CoMoO-12.4 after the long-term HER testing.

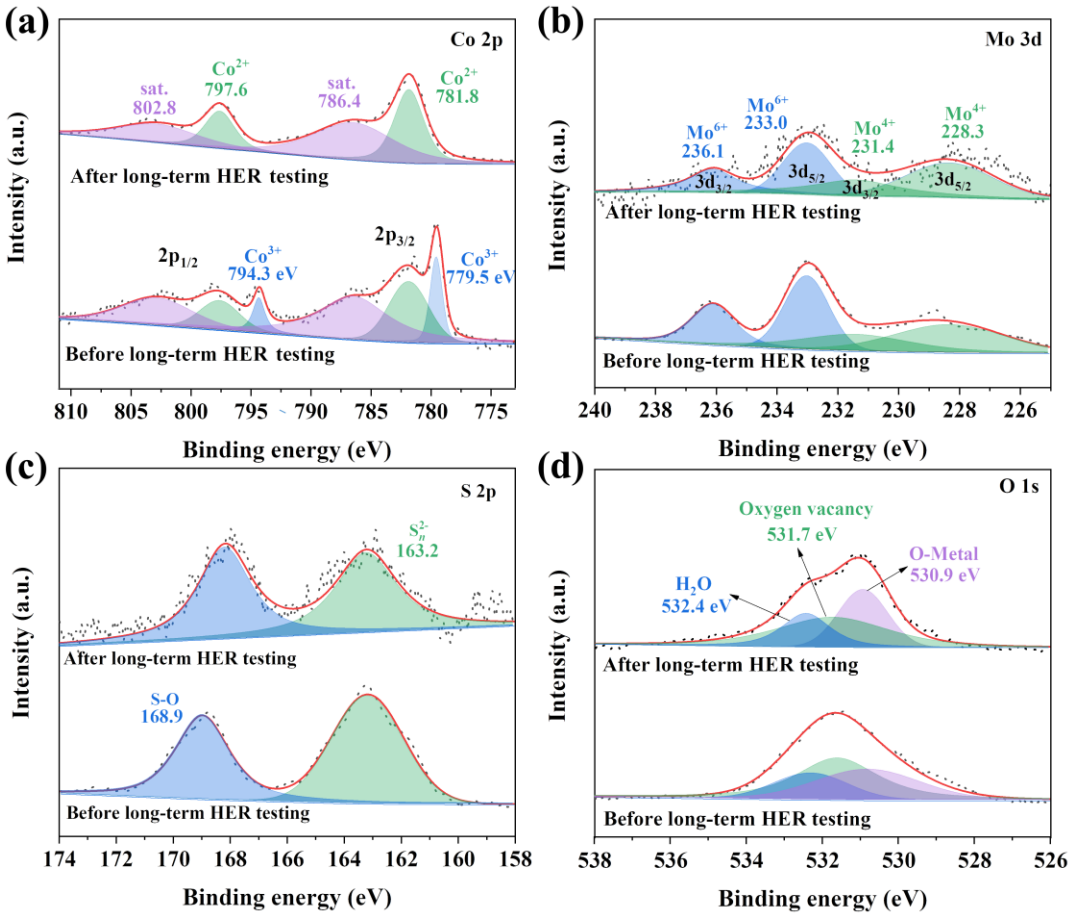

Fig. S8 The high-resolution spectra of (a) Co 2p, (b) Mo 3d, (c) S 2p and (d) O 1s of S-CoMoO-12.4 before and after the long-term HER testing.

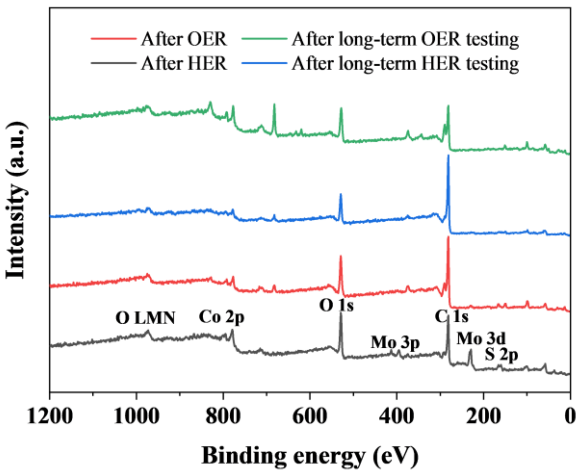

Fig. S9 The survey XPS spectra of S-CoMoO-12.4 after HER/OER and after long-term HER/OER testing.

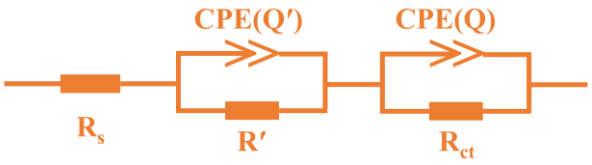

Fig. S10 The equivalent circuit model for electrochemical impedance tests. R_s, R', and R_{ct} represent the resistances of the equivalent series resistance, electrode porosity, and charge transfer, respectively. The constant phase angle element (CPE) represents the double-layer capacitance of a solid electrode in a real-world situation. And the R_s is generally acknowledged to contain the electrode resistance, electrolyte resistance, electrode/electrolyte interface resistance and collector/electrode contact resistance.

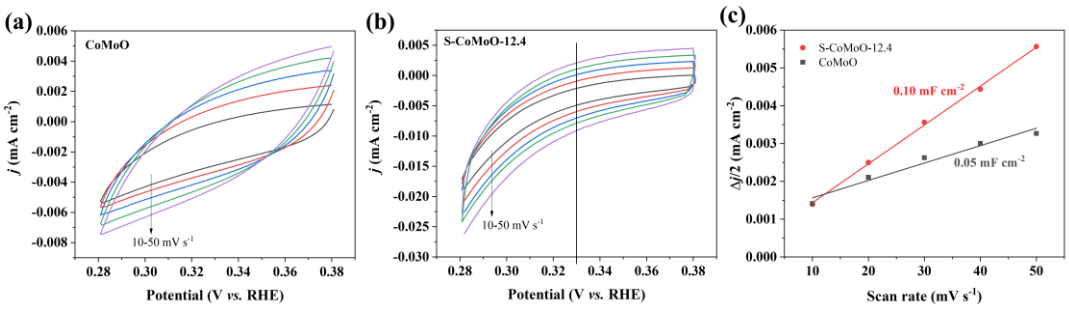

Fig. S11 CV curves measured at different scan rates from 10 to 50 mV s^{-1} in the region of 0.281 - 0.381 V in 1.0 M KOH for (a) CoMoO and (b) S-CoMoO-12.4; (c) CV current density versus sweep rate of different samples (the slope is equal to the C_{dl})

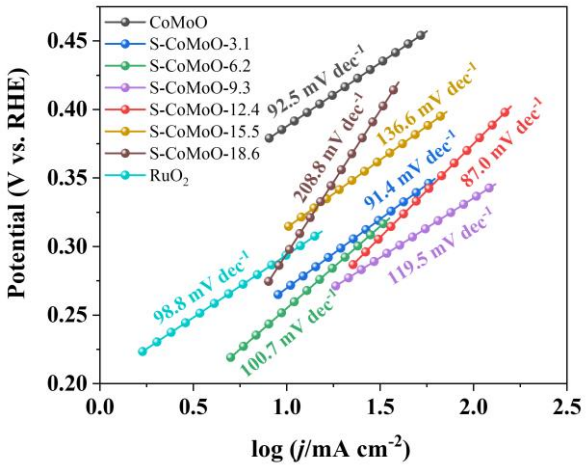

Fig. S12 Tafel curves (OER) of CoMoO, S-CoMoO-3.1, S-CoMoO-6.2, S-CoMoO-9.3, S-CoMoO-12.4, S-CoMoO-15.5, S-CoMoO-18.6, and RuO_2.

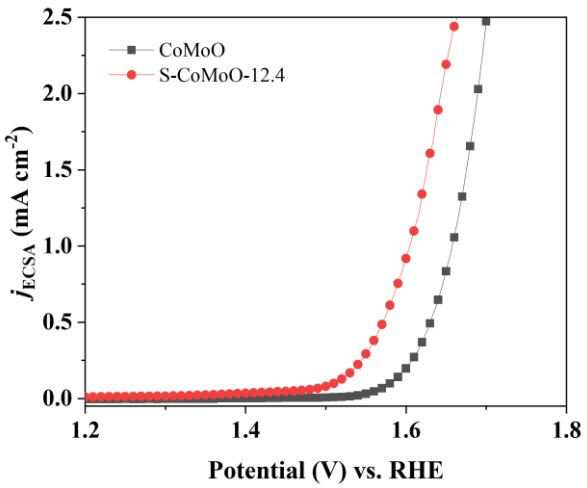

Fig. S13 The polarization curves (OER) for current density normalized to ECSA for CoMoO and S-CoMoO-12.4.

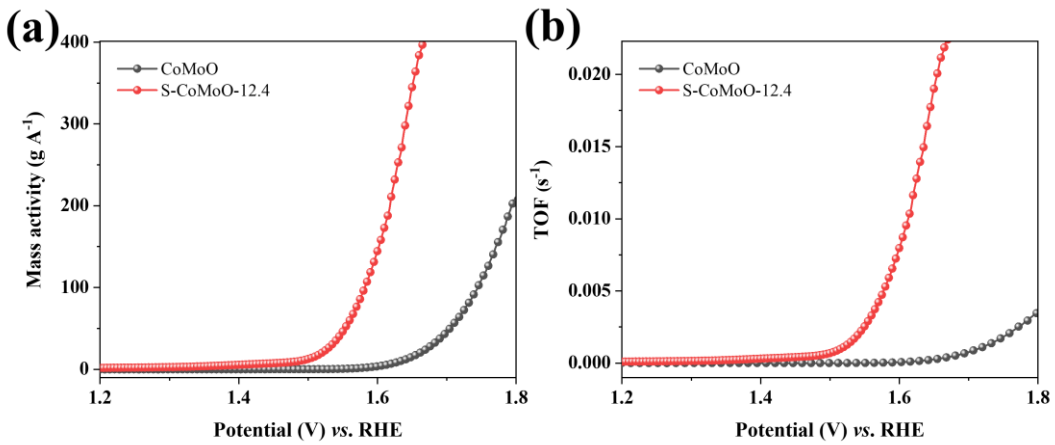

Fig. S14 The (a) mass activity and (b) turnover frequency of CoMoO and S-CoMoO-12.4.

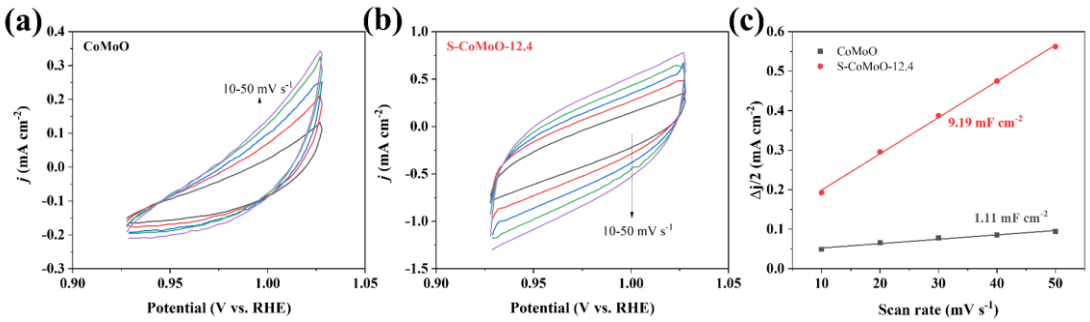

Fig. S15 CV curves measured at different scan rates from 10 to 50 mV s^{-1} in the region of 0.928 – 1.028 V in 1.0 M KOH for (a) CoMoO and (b) S-CoMoO-12.4; (c) CV current density versus sweep rate of different samples (the slope is equal to the C_{dl})

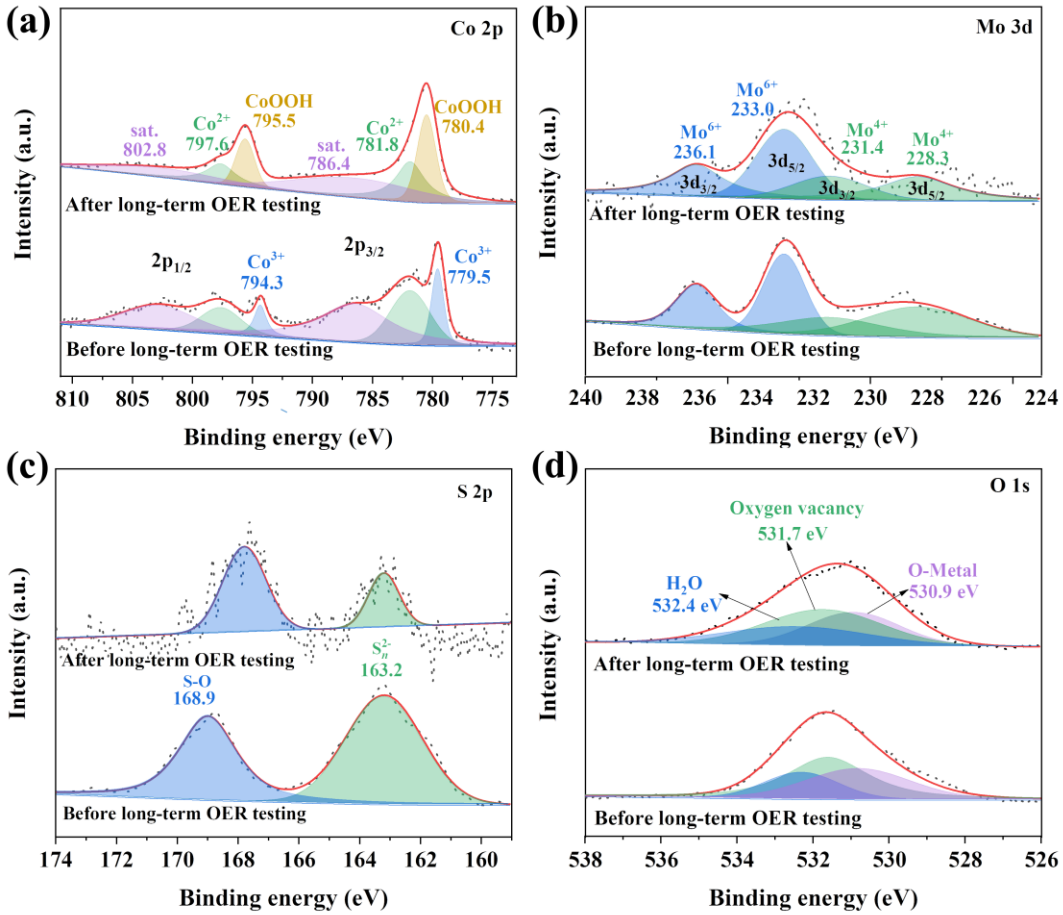

Fig. S16 The high-resolution spectra of (a) Co 2p, (b) Mo 3d, (c) S 2p and (d) O 1s of S-CoMoO-12.4 before and after the long-term OER testing.

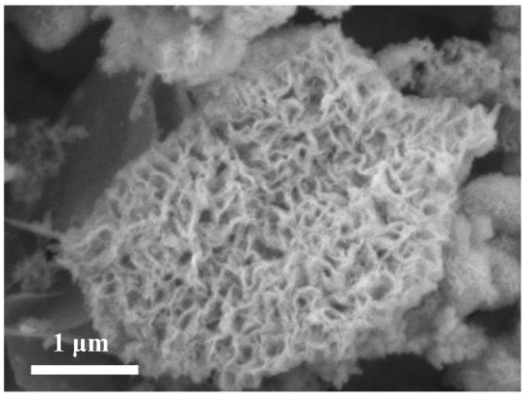

Fig. S17 SEM images of S-CoMoO-12.4 after the OER test.

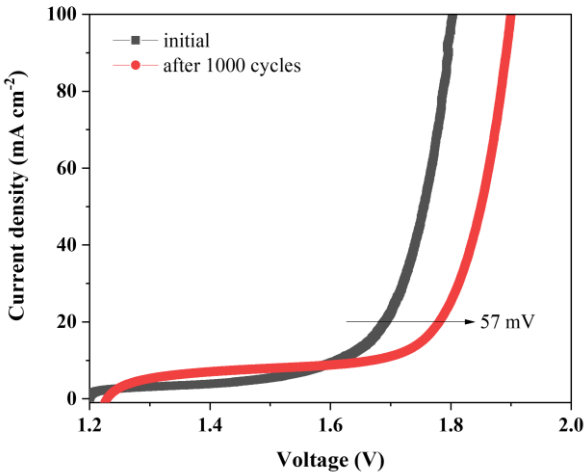

Fig. S18. LSV curves of S-CoMoO-12.4||S-CoMoO-12.4 e before and after the 1000 LSVs test.

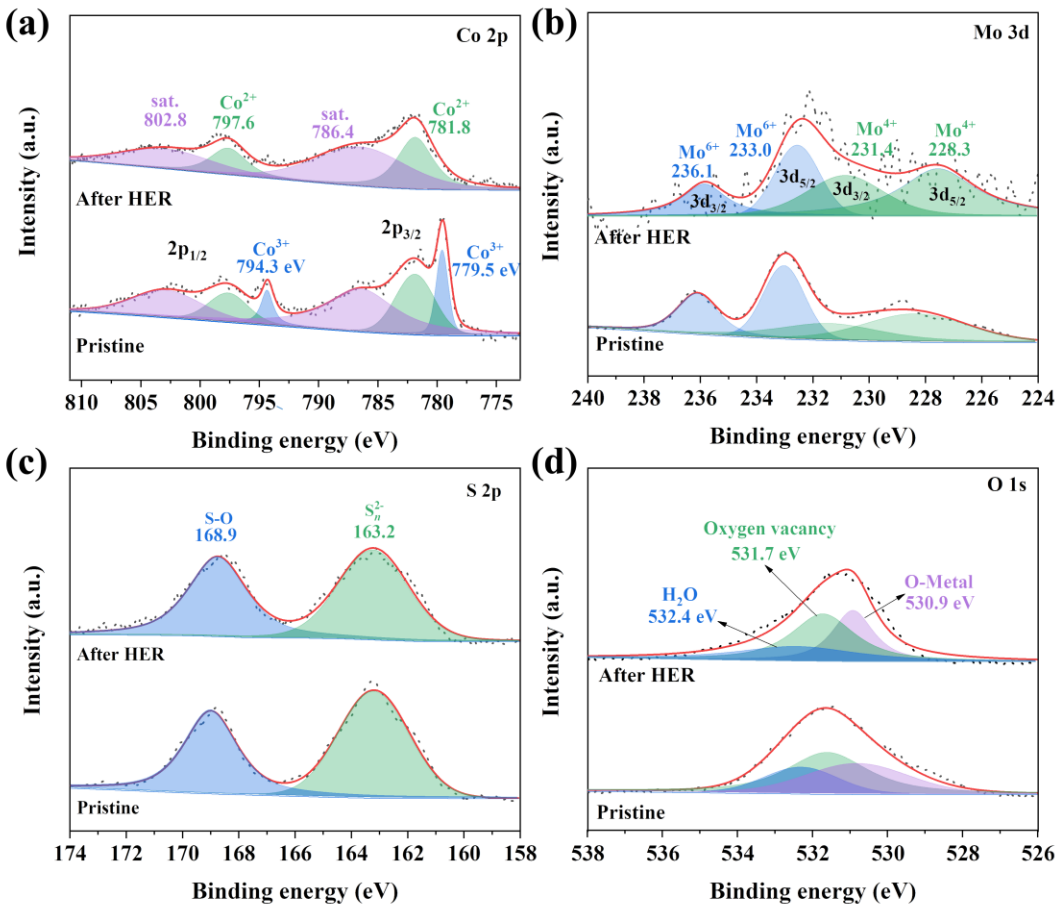

Fig. S19 The high-resolution spectra of (a) Co 2p, (b) Mo 3d, (c) S 2p and (d) O 1s of S-CoMoO-12.4 before and after the HER.

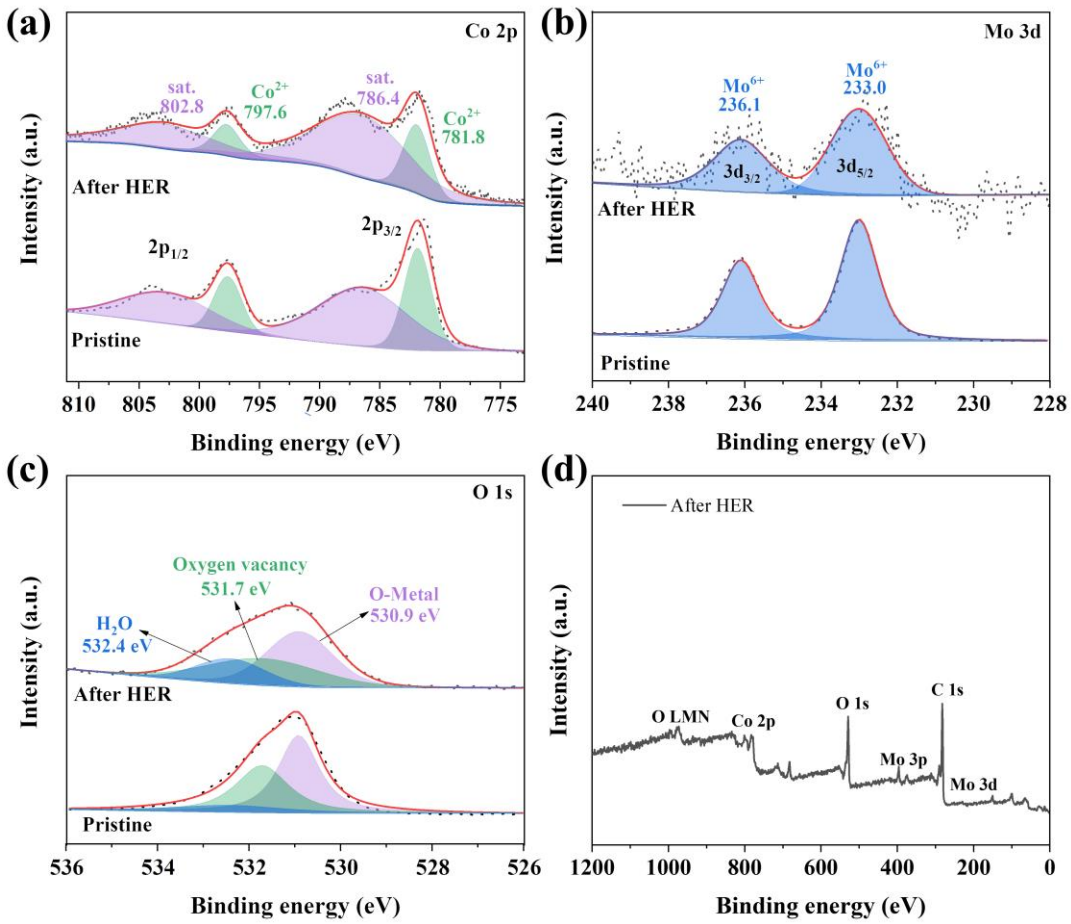

Fig. S20 The high-resolution spectra of (a) Co 2p, (b) Mo 3d and (c) O 1s of CoMoO before and after the HER; (d) survey spectrum of CoMoO after the HER.

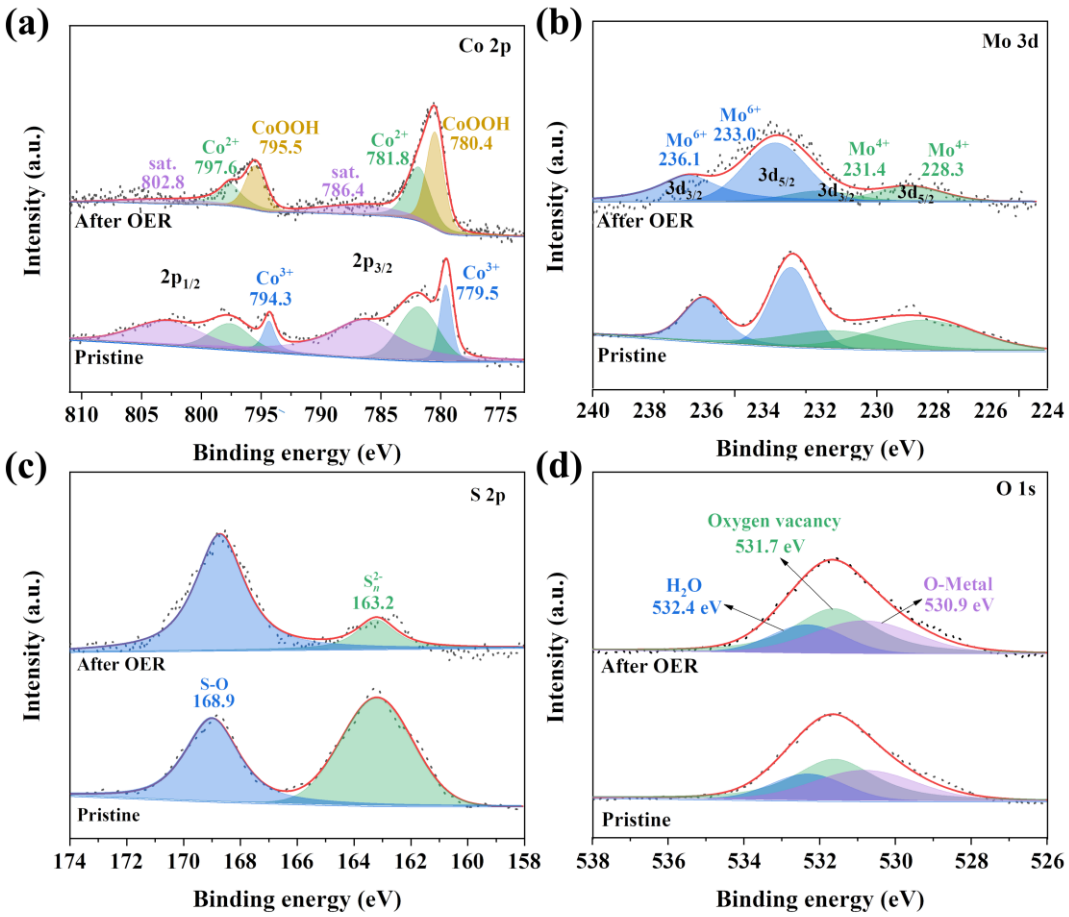

Fig. S21 The high-resolution spectra of (a) Co 2p, (b) Mo 3d, (c) S 2p and (d) O 1s of S-CoMoO-12.4 before and after the OER.

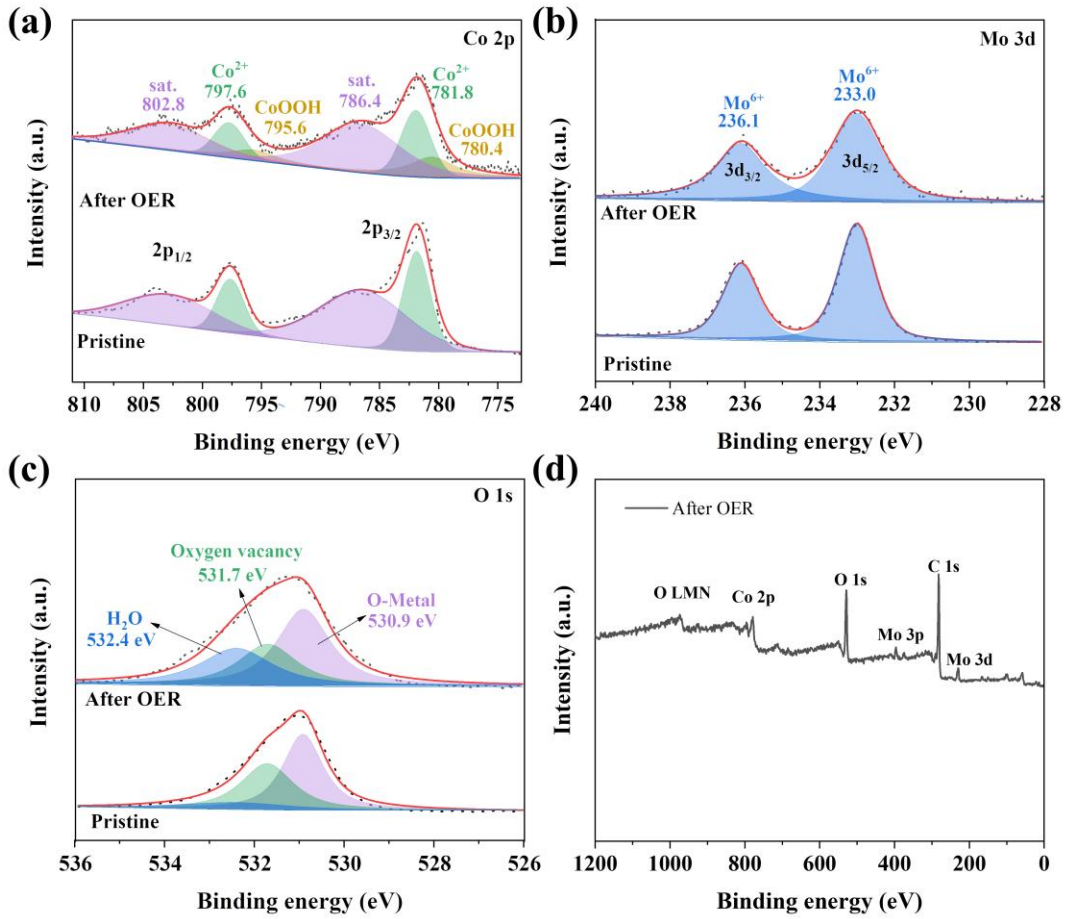

Fig. S22 The high-resolution spectra of (a) Co 2p, (b) Mo 3d and (c) O 1s of CoMoO before and after the HER; (d) survey spectrum of CoMoO after the OER.

Table S1 EDS analysis of the samples.

Sample	Element (atom %)			
	O	Co	Mo	S
CoMoO	67.2	19.1	13.7	0.0
S-CoMoO-3.1	56.8	27.5	12.2	3.5
S-CoMoO-6.2	66.2	16.5	10.2	7.1
S-CoMoO-9.3	71.5	11.4	9.1	8.0
S-CoMoO-12.4	70.7	8.9	6.8	13.6
S-CoMoO-15.5	68.9	9.7	6.9	14.5
S-CoMoO-18.6	67.2	9.9	8.0	14.9

Table S2 Parameters obtained from fitting the EIS spectra at HER.

Sample	R_s (Ω)	CPE (Q')		R'(Ω)	CPE (Q)		R_{ct} (Ω)
		Y_0' ($S \cdot s^{-n}$)	n′		Y_0 ($S \cdot s^{-n}$)	n	
CoMoO	1.76	0.28	0.55	0.21	0.07	0.88	10.03
S-CoMoO-12.4	1.38	2.13	0.55	0.62	0.81	0.97	2.66

Table S3 Parameters obtained from fitting the EIS spectra at OER.

Sample	R_s (Ω)	CPE (Q')		R'(Ω)	CPE (Q)		R_{ct} (Ω)
		Y_0' ($S \cdot s^{-n}$)	n′		Y_0 ($S \cdot s^{-n}$)	n	
CoMoO	1.62	4.60E-4	1.00	0.22	4.79 E-4	0.88	108.80
S-CoMoO-12.4	1.24	0.18	0.48	0.47	0.38	0.83	0.80

Table S4 Summary of recently reported non-noble metal based oxides electrocatalysts in alkaline conditions.

Catalyst	HER	OER	Cell voltage (V) at 10 mA cm^{-2}	Substrate	Ref.
	η_{10} (mV)	η_{10} (mV)			
S-CoMoO-12.4[a]	105	205	1.61	CFP	This work
CoV/CF-CWs[a]	118	204[c]	1.48	CF	[3]
CoFeO@BP[a]	88	266	1.58	GCE	[4]
AC-$SrIrO_3$[b]	139	300	1.59	GCE	[5]
S-CoO_x[a]	136	270	1.63	NF	[6]
CoFeZr oxides[a]	104	248	1.63	NF	[7]
Co-Cu-W oxide[b]	103	313	1.80	CF	[8]
SNCF-NRs[a]	232	370	1.68	GCE	[9]
CuCoO-NWs[a]	140	270[d]	1.61	NF	[10]
CoMnO[a]	45	200	1.50	NF	[11]
Ni-NiO/N-rGO	153[a]	240[b]	-	GCE	[12]
CoO_x@CN[a]	235	260	1.38	GCE	[13]
MoO_3/Ni–NiO	62	347[e]	1.55	CC	[14]
CoMoO@Co/GF	182	269	1.60	GF	[15]
P-CMO/NF-400	44	243	1.54	NF	[16]
CMO/NF	171	293	-	NF	[16]

Note: The η_{10} was overpotential (mV) at a current density of 10 mA cm^{-2}; CFP: carbon fiber paper; CF: copper foam; GCE: glassy carbon electrode; NF: nickel foam; CC: carbon cloth; GF: 3D graphite felt. [a-b] The HER performance of catalysts is measured in 1.0 and 0.1M KOH solution; [c-e] The overpotential at 20, 25 and 100 mA cm^{-2}.

Table S5 XPS peak positions and percent peak areas of fitted high-resolution spectra of Co 2p, Mo 3d, O 1s and S 2p for CoMoO and S-CoMoO-12.4.

Catalyst	Co $2p_{3/2}$		Mo $3d_{5/2}$		O 1s		S 2p		Co^{3+}/Co^{2+}	Mo^{4+}/Mo^{6+}	O_V/O_{lat}
	BE (eV)	Area (%)	BE (eV)	Area (%)	BE (eV)	Area (%)	BE (eV)	Area (%)			
CoMoO	781.8 (Co^{2+})	34.63	233.0 (Mo^{6+})	100	532.4 (H_2O)	12.42	-	-	0	0	0.79
	786.4 (sat.)	65.37			531.7 (O_v)	38.62					
					530.9 (O_{Lat})	48.96					
After HER	781.8 (Co^{2+})	22.45	233.0 (Mo^{6+})	100	532.4 (H_2O)	19.73	--	-	0	0	0.75
	786.4 (sat.)	77.55			531.7 (O_v)	34.58					
					530.9 (O_{Lat})	45.99					
After OER	781.8 (Co^{2+})	26.04	233.0 (Mo^{6+})	100	532.4 (H_2O)	28.86	-	-	0.66 ($CoOOH/Co^{2+}$)	0	0.59
	780.4 (CoOOH)	17.12			531.7 (O_v)	26.47					
	786.4 (sat.)	56.84			530.9 (O_{Lat})	44.67					
S-CoMoO-12.4	781.8 (Co^{2+})	30.41	233.0 (Mo^{6+})	50.27	532.4 (H_2O)	24.36	168.9 (S-O)	43.89	0.50	0.99	1.14
	779.5 (Co^{3+})	15.08	228.3 (Mo^{4}+)	49.73	531.7 (O_v)	40.25	163.2 (S_n^{2-})	56.11			
	786.4 (sat.)	54.51			530.9 (O_{Lat})	35.39					
After HER	781.8 (Co^{2+})	36.99	233.0 (Mo^{6+})	37.25	532.4 (H_2O)	25.77	168.8 (S-O)	52.29	0	1.68	1.43
	786.4 (sat.)	63.01	228.3 (Mo^{4}+)	62.75	531.7 (O_v)	43.62	163.2 (S_n^{2-})	47.71			
	779.5 (Co^{3+})	-			530.9 (O_{Lat})	30.61					
After OER	781.8 (Co^{2+})	37.28	233.0 (Mo^{6+})	78.04	532.4 (H_2O)	19.87	168.7 (S-O)	83.31	1.21 ($CoOOH/Co^{2+}$)	0.28	1.40
	780.4 (CoOOH)	45.29	228.3 (Mo^{4}+)	21.96	531.7 (O_v)	46.78	163.2 (S_n^{2-})	16.69			
	786.4 (sat.)	17.43			530.9 (O_{Lat})	33.35					

References

1 K. Elbert, J. Hu, Z. Ma, Y. Zhang, G. Y. Chen, W. An, P. Liu, H. S. Isaacs, R. R. Adzic and J. X. Wang, *ACS Catal.*, 2015, **5**, 6764-6772.

2 J. Hu, C. X. Zhang, L. Jiang, H. Lin, Y. M. An, D. Zhou, M. K. H. Leung and S. H. Yang, *Joule*, 2017, **1**, 383-393.

3 Z. T. Li, J. Yang, Z. Chen, C. Y. Zheng, L. Q. Wei, Y. C. Yan, H. Hu, M. B. Wu and Z. P. Hu, *Adv. Funct. Mater.*, 2021, **31**, 2008822.

4 X. Y. Li, L. P. Xiao, L. Zhou, Q. C. Xu, J. Weng, J. Xu and B. Liu, *Angew. Chem. Int. Ed.*, 2020, **59**, 21106-21113.

5 J. Yu, X. H. Wu, D. Q. Guan, Z. W. Hu, S. C. Weng, H. N. Sun, Y. F. Song, R. Ran, W. Zhou, M. Ni and Z. P. Shao, *Chem. Mater.*, 2020, **32**, 4509-4517.

6 X. X. Yu, Z. Y. Yu, X. L. Zhang, P. Li, B. Sun, X. C. Gao, K. Yan, H. Liu, Y. Duan, M. R. Gao, G. X. Wang and S. H. Yu, *Nano Energy*, 2020, **71**, 104652.

7 L. L. Huang, D. W. Chen, G. Luo, Y. R. Lu, C. Chen, Y. C. Zou, C. L. Dong, Y. F. Li and S. Y. Wang, *Adv. Mater.*, 2019, **31**, 1901439.

8 D. D. Gao, R. J. Liu, J. Biskupek, U. Kaiser, Y. F. Song and C. Streb, *Angew. Chem. Int. Ed.*, 2019, **58**, 4644-4648.

9 Y. L. Zhu, W. Zhou, Y. J. Zhong, Y. F. Bu, X. Y. Chen, Q. Zhong, M. L. Liu and Z. P. Shao, *Adv. Energy Mate.*, 2017, **7**, 1602122.

10 M. Kuang, P. Han, Q. H. Wang, J. Li and G. F. Zheng, *Adv. Funct. Mater.*, 2016, **26**, 8555-8561.

11 J. Li, Y. C. Wang, T. Zhou, H. Zhang, X. H. Sun, J. Tang, L. J. Zhang, A. M. Al-Enizi, Z. Q. Yang and G. F. Zheng, *J. Am. Chem. Soc.*, 2015, **137**, 14305-14312.

12 X. Liu, W. Liu, M. Ko, M. Park, M. G. Kim, P. Oh, S. Chae, S. Park, A. Casimir, G. Wu and J. Cho, *Adv. Funct. Mater.*, 2015, **25**, 5799-5808.

13 H. Y. Jin, J. Wang, D. F. Su, Z. Z. Wei, Z. F. Pang and Y. Wang, *J. Am. Chem. Soc.*, 2015, **137**, 2688-2694.

14 X. Li, Y. Wang, J. Wang, Y. Da, J. Zhang, L. Li, C. Zhong, Y. Deng, X. Han and W. Hu, *Adv. Mater.*, 2020, **32**, 2003414.

15 L. Lei, Z. Yin, D. L. Huang, Y. S. Chen, S. Chen, M. Cheng, L. Du and Q. H. Liang, *J. Colloid Interf. Sci.*, 2022, **612**, 413-423.

16 J. Wang, J. Hu, C. Liang, L. M. Chang, Y. C. Du, X. J. Han, J. M. Sun and P. Xu, *Chem. Eng. J.*, 2022, **446**, 137094.